

Equation of State for a Complex Plasma from Recursive Bayesian Estimation

Neil P. Oxtoby,^{*} Elias J. Griffith, Céline Durniak, Jason F. Ralph, and Dmitry Samsonov

*Department of Electrical Engineering and Electronics,
University of Liverpool, Liverpool, L69 3GJ, United Kingdom*

(Dated: 5 December 2012)

We demonstrate that high-precision object tracking using recursive Bayesian estimation significantly improves empirical estimates for the equation of state of an experimental two-dimensional complex plasma, which we exposed to a series of electrostatic pulses to excite shock waves of different intensities. The estimate for the adiabatic index approaches that of a monatomic ideal gas ($\gamma = 5/3$), verifying a common assumption in the analysis of complex plasmas. Lower-precision dust kinematics from particle tracking velocimetry introduced a bias in the estimate of the adiabatic index.

PACS numbers: 52.27.Lw, 52.35.Fp, 52.35.Tc, 51.30.+i

Keywords: complex plasma, dusty plasma, equation of state, Hugoniot, state estimation, tracking, Kalman filter, Bayesian

An equation of state, such as the ideal gas law, is a mathematical relation between physical constants and macroscopically observable properties of a single phase of a system in equilibrium [1]. Equations of state are path-independent, and so can be explored by changing a system along any convenient intraphase path in state space between equilibria. Interphase paths include a phase transition — a discontinuous change in one or more system properties. For example, the significant increase in volume when liquid water evaporates. Nonequilibrium paths, whether intraphase or interphase, can also be used to infer an equation of state, but an assumption is required to link the nonequilibrium states to the equilibrium states. This is the case in shock wave physics where otherwise unreachable high pressure and high density regions of state space are explored. Pressure–density curves from shock experiments do not provide enough thermodynamic information to infer an equation of state [2], but can be used to fit parameters in an assumed equation of state. We explore parameter fitting in the ideal gas equation of state, applied to a complex plasma.

A laboratory complex plasma consists of plastic microspheres suspended in a low-density ionized gas. The microspheres are often referred to as *dust* particles in analogy with dusty plasmas observed in astronomy [3, 4]. Fast-moving electrons and relatively slow-moving ions in the plasma deposit a net negative charge on the dust, which repel each other via a screened Coulomb force (Yukawa or Debye-Hückel) [5]. Condensed-matter-like behaviour results when the dust is electrostatically confined, with the dust mimicking microscopic constituents of a fluid (individual molecules/atoms), yet being observable on a macroscopic scale (even to the naked eye). The space between dust particles is occupied by a rarefied gas, so these dusty plasma structures experience very little damping, and are therefore considered to be representative models of liquids and solids [6]. Dusty plasmas are thus an excellent vehicle for exploring the microscopic kinematics of melting processes and crystal formation.

Thermodynamic properties of the dust can be calculated from the kinematics of the individual particles. Particle positions extracted from images determine the dust density via Voronoi analysis [7, 8], and particle velocities determine the kinetic temperature [9, 10]. Dust kinematics are normally estimated using particle tracking velocimetry (PTV) [11], where *average* velocity $\vec{v}_{\text{PTV}}(t+T/2) = [\vec{x}(t+T) - \vec{x}(t)]/T$ is calculated from consecutive position measurements $\vec{x}(t+T)$, $\vec{x}(t)$, which are extracted from a sequence of images taken with a high-speed camera at a frame rate of $1/T$ (typically 500–1000 frames per second). The velocity calculated in this way is subject to two sources of inaccuracy: position uncertainty in the measurement, and nonzero acceleration. For very high frame rates $T \rightarrow 0$, v_{PTV} is limited by position uncertainty, which is due to finite pixel size and noise in the camera sensor [12, 13]. These limitations can lead to artefacts in results calculated from PTV-estimated kinematics. Recursive state estimation (also known as *object tracking* [14, 15]) has been employed to estimate the kinematics of complex plasma particles [9, 16]. Object tracking algorithms filter noisy measurements via a set of equations to produce estimates of the *instantaneous* kinematics which are resilient to the limitations discussed above. The most ubiquitous recursive Bayesian estimator is the Kalman filter [17].

In this work we employ object tracking using an interacting multiple model tracker [9] based on Kalman filtering (KF) to generate thousands of simultaneous particle tracks from shock wave experiments on a two-dimensional (2D) complex plasma. We use Rankine-Hugoniot relations [18] to calculate Hugoniot curves arising from the estimated kinematics, and interpret the results using the ideal gas equation of state. We compare our KF results with those from PTV, which does not account for the non-negligible particle acceleration in shock wave experiments, and find that PTV introduces a systematic error that gives rise to a bias in the estimated equation of state. Object tracking can incorporate parti-

cle acceleration in one of two ways: either by modelling known interparticle forces, or by including acceleration in the recursive estimation algorithm along with position and velocity. Multiple forces govern the dust dynamics [5], including Yukawa (particle interactions), external (confinement and excitation), and friction (plasma drag) forces. For a well-characterized system with known particle charge, Debye length, damping rate, particle mass, etc., the total force on each particle is calculable from the positions and velocities of all particles. Such known accelerations can be exploited by a state estimation filter to improve the accuracy of particle tracks [9]. However, complete characterization of a complex plasma is extremely challenging. Fortunately, even in the absence of exact knowledge of the physical parameters, object tracking allows the acceleration of the particles to be estimated recursively — along with position and velocity — thereby improving force estimates. This is the situation considered here.

Equation of State — The most common thermodynamic relation for compressible flow is the ideal gas law, which can be written in terms of the following specific (per unit mass) quantities: pressure p , internal energy e and density n as

$$p = (\gamma - 1)en, \quad (1)$$

where γ is the adiabatic index. In the case of an ideal gas undergoing an isentropic process (reversible adiabatic process), γ is the ratio of specific heats at constant pressure and constant volume. Deviations from the ideal gas law were first considered by van der Waals in 1873 to account for finite particle size and molecular interactions [19]. However, the ideal gas law can be applied to non-ideal gases with sufficient accuracy in many cases [20].

Here we explore the $p(e, n)$ relation in a non-perturbative manner by exciting a series of shocks of different magnitudes in the dust [10, 21, 22]. A normal shock wave is one where the shock front is normal to the direction of propagation, and the bulk flow is one-dimensional. In the frame of a normal shock moving at speed u_S , the Rankine-Hugoniot shock relations for conservation of mass, momentum and energy across the shock front are, respectively, [18]

$$n_2 \tilde{u}_2 = n_1 \tilde{u}_1 \quad (2a)$$

$$\tilde{p}_2 + n_2 \tilde{u}_2^2 = \tilde{p}_1 + n_1 \tilde{u}_1^2 \quad (2b)$$

$$e_2 + \frac{1}{2} \tilde{u}_2^2 + \frac{\tilde{p}_2}{n_2} = e_1 + \frac{1}{2} \tilde{u}_1^2 + \frac{\tilde{p}_1}{n_1}, \quad (2c)$$

where $u_{1/2} = u_S - \tilde{u}_{1/2}$ denotes the particle speed downstream/upstream (ahead/behind) from the shock in the laboratory frame and the moving frame is denoted with a tilde as $\tilde{u}_{1/2}$. Specific density n and internal energy e are equal in the laboratory frame and the moving frame, but pressure has a kinetic component. We found this to be

small ($< 5\%$) compared to the Yukawa pressure (shear stress [23]) so that $\tilde{p} \approx p$. Equation (2c) is known as *the Hugoniot* [24]. Using equation (1) to eliminate internal energy from equation (2c), and combining with equation (2b), we can write [18]

$$\xi(\eta) = \frac{\eta(\gamma + 1) - (\gamma - 1)}{(\gamma + 1) - \eta(\gamma - 1)}, \quad (3)$$

where $\xi \equiv \tilde{p}_2/\tilde{p}_1$ is the shock strength and $\eta \equiv n_2/n_1$ is the compression ratio across the shock. A least-squares fit of the experimental results to equation (3) yields an estimate of γ , and hence an equation of state for the shocked dust in the form of equation (1).

Polytropic index — With the ideal gas law as the equation of state, the polytropic index g can be used to describe the physical nature of a process that changes an initial state (downstream p_1, n_1) to the final state (upstream p_2, n_2). Polytropic processes follow $p/n^g = C$ [4], which describes a curve in the pressure-density diagram, with g and constant C defining a solution for the pressure/density changes linking the initial and final states. Equating initial and final states (both equal to C) then combining with ξ and η then solving for g allows the polytropic index to be expressed in terms of ξ and η as

$$g = \frac{\ln(\xi)}{\ln(\eta)}, \quad (4)$$

where $g = 0$ indicates an isobaric process, $g = 1$ is an isothermal process and $g = \gamma$ is an adiabatic process.

Experiment — The experiment involves levitating a 2D array of microspheres 10mm above the floor of an Argon-filled chamber pressurized to 2.05Pa. The spheres (9.2 μ m diameter) were then allowed to settle into a well-spaced crystalline structure, forming a “plasma crystal” [22] which is visible to the naked eye when illuminated by a laser sheet (figure 1). These dust particles each hold an approximate charge of $Q = 16000e$ and have a Debye length of $\lambda_D = 1.0$ mm [25, 26]. Shock waves were created by an electrode located to one side of the visible area, which was pulsed for 2 seconds with a voltage selected from -20 V to -50 V in 5V steps. The crystal was allowed to reset between each run (requiring approximately 100 seconds). The experiment was repeated at each voltage level to reduce the impact of local variation in crystal structure that can form on reset. The dust was imaged from above by a grayscale camera at 500 frames per second for 1.2 seconds, and the resulting images processed by PTV and our Kalman-filter-based tracking algorithm to obtain the dust kinematics. Further details of the experimental apparatus required to achieve this is described in references [22] and [27]. An example snapshot image of the dust, enhanced for presentation with enlarged dots and false color, is shown in figure 1 with a zoomed inset around the shock front. The symmetry inherent in normal shocks permits a 1D description of

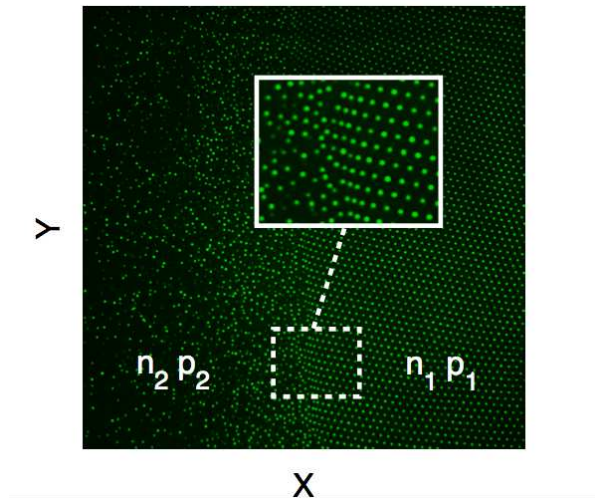


FIG. 1. Typical overhead image with zoomed inset, enhanced for presentation (enlarged dots, false color). The visible area is 32.8mm square imaged at a resolution of 1024×1024 pixels.

the thermodynamics. The *profile* values were calculated as robust average quantities (median, median absolute deviation) in each of 50 bins equally spaced along the X axis, which spanned the Y axis. The density and pressure profiles were used to generate a $p(n)$ plot below. Density is the inverse of the Voronoi cell area [7, 8], and pressure is calculated as shear stress, i.e., the X -component of the 2D stress tensor [23].

Our investigation proceeded as follows. The shock front was identified as a peak in the density profile evolution (see figure 2), from which the shock position and speed was determined. The upstream and downstream quantities in the Rankine-Hugoniot shock-jump relations were selected from 0.656mm (1 bin) behind the shock front and 3.28mm (5 bins) ahead. We needed to look further ahead to overcome the finite width of the shock front (an ideal shock would have vanishing width). Results were also sensitive to the chosen upstream distance due to structure a few millimetres behind the shock (see multi-shock discussion below).

A principal Hugoniot $p(n)$ requires repeated shock experiments of different magnitudes, sharing a common initial condition. Reliably reproducing the same initial condition for a dust crystal is extremely difficult, if not impossible. For this reason the data was post-selected from the densest cluster of initial conditions and constrained to lie within 1% of the cluster centroid. This is illustrated in figure 3 where the post-selected downstream data points are shown as blue dots and all others as red crosses. The inset of figure 3 also shows the post-selected upstream data. From 13 similar experimental runs, 118 total data points were generated, of which 26 were post-selected.

Results — Figure 2 clearly shows two density peaks: one leading (black) and one trailing (white). Such multi-

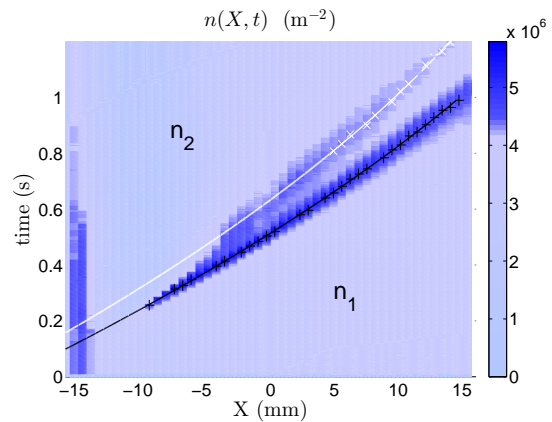


FIG. 2. Evolution of the dust particle number density profile $n(X, t)$. The density peaks (crosses) clearly shows the propagating shock wave (black), with an additional trailing shock (white). Quadratic least-squares fits are shown.

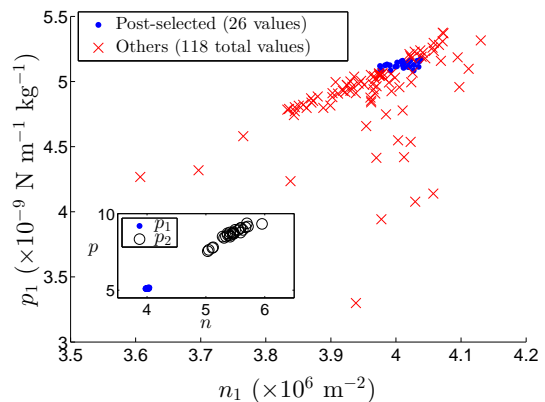


FIG. 3. Initial pressure and density (n_1, p_1) for each run: blue dots survived post-selection (see text). **Inset:** Pressure-density diagram showing all post-selected results: initial (blue dots) and final states (black circles).

shock structures [28] can be described by a sequence of jump relations of the same form as (2), and are stable when each wave travels at least as fast as the trailing waves (so the lead shock is not overtaken). This was the case here, where least-squares fits for the shock (S) and trailing (T) peak positions determined the wave speeds (mm/s) to be $u_S(t) = -17.2t + 43.7$ and $u_T(t) = -8.4t + 33.0$. The shock front is detectable after 0.24 seconds, with the trailing shock resolvable after 0.45 seconds.

Figure 4 shows shock strength vs. compression for both PTV and KF (object tracking). Least-squares fits to equation (3) determined the estimated adiabatic index for each approach. We found $\gamma_{\text{KF}} = 1.67 \pm 0.01$, which is consistent with that of a monatomic ideal gas $\gamma_{\text{Ideal}} = 5/3 = 1.6\bar{6}$. By contrast, PTV overestimated the value at $\gamma_{\text{PTV}} = 1.79 \pm 0.01$. The following discussion explores the reason why PTV overestimates γ from

the ξ - η plot. The post-selection renders the downstream data not culpable since variation is minimal by design. So, ξ and η are directly proportional to \tilde{p}_2 and n_2 , respectively. Dust pressure (and hence ξ) is dominated by the Yukawa interaction, which is non-linear in interparticle spacing r (e.g., see [9]), and particularly sensitive to errors in r . When averaged, these errors propagate through the non-linearities to create a biased *overestimate* for the pressure, thereby shifting erroneous results upward in the ξ - η plane. Dust density (and hence η) is easily *underestimated* when excited dust particles intermittently leave the plane of illumination. The object tracking process provides a robust way to maintain tracks for these particles that PTV does not. The reduction of η due to such track loss shifts erroneous results to the left in the ξ - η plane. In figure 4 the PTV result is above and left of the KF result (which may lie above or on the true result).

We determined the polytropic index of the shocked dust from our KF results via the mean value of equation (4). We found $g_{KF} = 1.71 \pm 0.07$ which satisfies $g \approx \gamma$, thereby demonstrating that shocks in a dusty plasma (which here behaves as an ideal gas) constitute an adiabatic process. Thus, our investigation experimentally verifies the expectation that shocks in an ideal gas are an adiabatic process [4]. Conventionally this is often *assumed* to hold, at least as an approximation, whereas we have verified the validity of this assumption experimentally.

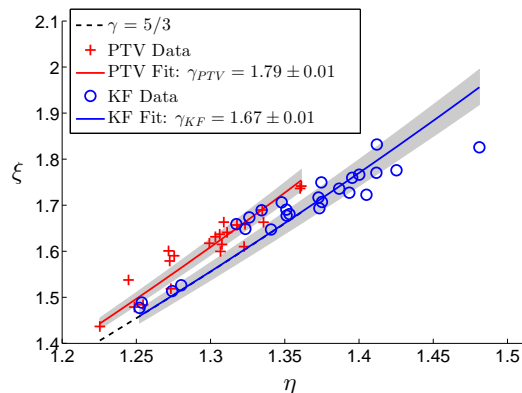


FIG. 4. Shock strength vs. compression ratio for PTV and KF. Least-squares fits to equation (3) give the adiabatic index γ , with 3σ confidence regions in each case shown in gray.

Figure 5 shows the shock Hugoniot [29, 30], where the shock velocity u_S is linearly related to the upstream velocity u_2 behind the shock front: $u_S = Su_2 + C_0$. Here C_0 is the zero-pressure bulk speed of sound (speed of sound in an unshocked sample), and S is a dimensionless constant of proportionality for the linear fit. The PTV and KF methods estimate C_0 to be 26.8 mm/s and 21.8 mm/s, respectively. These values are in line with the 25 mm/s and 28 mm/s speeds of sound observed in [31] and

[32] via different techniques. The very low speeds are due to the extreme softness of the dust crystal, which is due to the large interparticle spacing in comparison with the particle size [31]. (Recall that the particles shown in figure 1 have been enlarged for clarity.) In the fits of figure 5, the coefficient of determination R^2 showed that the KF data ($R^2 = 0.64$) followed the expected linear trend far better than the relatively scattered PTV data ($R^2 = 0.27$). While there is still some way to go ($R^2 = 1$ is a perfect fit), this result further increases our confidence in using object tracking methods to analyse dusty plasma experiments, rather than the prevailing PTV approach.

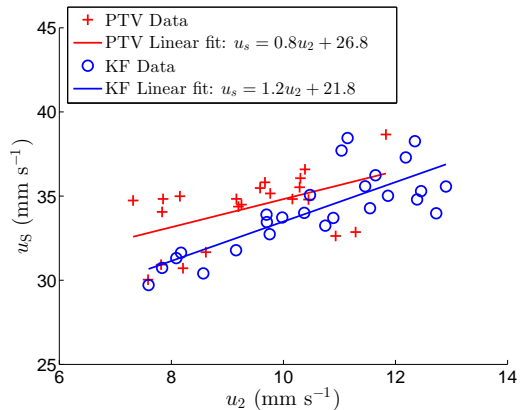


FIG. 5. Shock front speed vs. upstream particle speed (*Shock Hugoniot*) for both PTV and KF (object tracking).

Conclusion — We performed shock experiments in a two-dimensional dusty plasma. This model system for exploring the microscopic dynamics of molecular systems allowed us to calculate thermodynamic variables for the dust (pressure, density) directly from the kinematics of the myriad dust particles. The kinematics were estimated using two techniques: a recursive Bayesian state estimation technique (object tracking), and particle tracking velocimetry (the standard approach in complex plasma physics). Conservation laws known as Rankine-Hugoniot equations were combined with the ideal gas law to estimate the adiabatic index of the dust, which verified two common assumptions: that a dusty plasma can be considered as an ideal gas, and that a shock wave in an ideal gas is an adiabatic process.

We found that PTV analysis overestimated the adiabatic index (and hence produced an inaccurate estimate for the equation of state), due to a systematic error introduced when the errors from PTV are used in the nonlinear equations. This reinforces that object tracking produces reliable dust particle tracks [9] and should be used when analyzing complex plasma physics experiments.

Acknowledgments — This work was supported by the Engineering and Physical Sciences Research Council of the United Kingdom through grant number

EP/G007918. N.P.O. acknowledges use of high-throughput computational resources provided by the eScience team at the University of Liverpool. The experiments were performed by D.S., who passed away during the final stages of preparation of this paper. Dmitry will be sorely missed by the plasma physics community.

* Current address: Department of Computer Science, University College London, Gower Street, WC1E 6BT, London, UK

- [1] L. D. Landau and E. M. Lifshitz, *Statistical Mechanics*, 2nd ed. (Pergamon, Oxford, 1969).
- [2] M. Cowperthwaite, *American Journal of Physics* **34**, 1025 (1966).
- [3] R. L. Merlino and J. A. Goree, *Physics Today* **57**, 32 (2004).
- [4] J. A. Newbury, C. T. Russell, and G. M. Lindsay, *Geophys. Res. Lett.* **24**, 1431 (1997).
- [5] P. K. Shukla and B. Eliasson, *Rev. Mod. Phys.* **81**, 25 (2009).
- [6] G. E. Morfill and A. V. Ivlev, *Rev. Mod. Phys.* **81**, 1353 (2009).
- [7] G. M. Voronoi, *J. Reine Angew. Math.* **134**, 198 (1908).
- [8] F. Aurenhammer, *ACM Computing Surveys* **23**, 345 (1991).
- [9] N. P. Oxtoby, J. F. Ralph, C. Durniak, and D. Samsonov, *Physics of Plasmas* **19**, 013708 (2012).
- [10] D. Samsonov and G. Morfill, *Plasma Science, IEEE Transactions on* **36**, 1020 (2008).
- [11] Y. Stegeman, *Particle Tracking Velocimetry* (Technische Universiteit Eindhoven, 1995).
- [12] Y. Feng, J. Goree, and B. Liu, *Review of Scientific Instruments* **78**, 053704 (2007).
- [13] Y. Feng, J. Goree, and B. Liu, *Review of Scientific Instruments* **82**, 053707 (2011).
- [14] Y. Bar-Shalom, X. Li, and T. Kirubarajan, *Estimation with Applications to Tracking and Navigation* (Wiley-Interscience, New York, 2001).
- [15] J. F. Ralph, "Target Tracking," in *Encyclopedia of Aerospace Engineering*, Vol. 5: Dynamics and Control, edited by R. Blockley and W. Shyy (John Wiley & Sons, Inc., 2010) Chap. 251.
- [16] V. Hadziavdic, F. Melandsø, and A. Hanssen, *Physics of Plasmas* **13**, 053504 (2006).
- [17] R. E. Kalman, *Journal of Basic Engineering* **82**, 35 (1960).
- [18] J. W. Bond, Jr., K. M. Watson, and J. A. Welch, Jr., *Atomic Theory of Gas Dynamics*, Addison-Wesley Series in Aerospace Science, Vol. 633 (Addison-Wesley, Reading, Massachusetts, 1965).
- [19] J. D. van der Waals, *Over de Continuïteit van den Gas- en Vloeistofoestand*, Ph.D. thesis, Leiden (1873).
- [20] B. P. Pandey, *Phys. Rev. E* **69**, 026410 (2004).
- [21] D. Samsonov, G. Morfill, H. Thomas, T. Hagl, H. Rothermel, V. Fortov, A. Lipaev, V. Molotkov, A. Nefedov, O. Petrov, A. Ivanov, and S. Krikalev, *Phys. Rev. E* **67**, 036404 (2003).
- [22] D. Samsonov, S. K. Zhdanov, R. A. Quinn, S. I. Popel, and G. E. Morfill, *Phys. Rev. Lett.* **92**, 255004 (2004).
- [23] Z. Donkó, J. Goree, and P. Hartmann, *Phys. Rev. E* **81**, 056404 (2010).
- [24] L. F. Henderson, "General Laws for Shock Waves Through Matter," in *Handbook of Shock Waves*, Vol. 1, edited by G. Ben-Dor, O. Igra, T. Elperin, and A. Lifshitz (Academic Press, 2001) Chap. 2.
- [25] P. Harvey, C. Durniak, D. Samsonov, and G. Morfill, *Phys. Rev. E* **81**, 057401 (2010).
- [26] C. Durniak, D. Samsonov, N. P. Oxtoby, J. F. Ralph, and S. Zhdanov, *Plasma Science, IEEE Transactions on* **38**, 2412 (2010).
- [27] D. Samsonov, S. Zhdanov, and G. Morfill, *Phys. Rev. E* **71**, 026410 (2005).
- [28] G. E. Duvall and R. A. Graham, *Rev. Mod. Phys.* **49**, 523 (1977).
- [29] M. H. Rice, R. G. McQueen, and J. M. Walsh, in *Advances in Research and Applications*, Solid State Physics, Vol. 6, edited by F. Seitz and D. Turnbull (Academic Press, 1958) pp. 1 – 63.
- [30] K. Nagayama, Y. Mori, K. Shimada, and M. Nakahara, *Journal of Applied Physics* **91**, 476 (2002).
- [31] Y. Feng, J. Goree, and B. Liu, *Physical Review Letters* **109**, 185002 (2012).
- [32] M. Schwabe, K. Jiang, S. Zhdanov, T. Hagl, P. Huber, A. V. Ivlev, A. M. Lipaev, V. I. Molotkov, V. N. Naumkin, K. R. Sütterlin, H. M. Thomas, V. E. Fortov, G. E. Morfill, A. Skvortsov, and S. Volkov, *EPL (Europhysics Letters)* **96**, 55001 (2011).